

RESEARCH LETTER

10.1002/2017GL076287

Key Points:

- Aftershocks are driven by afterslip
- The model predicts an apparent propagation velocity scales as 1/time
- We relate the propagation velocity to the physical parameters of the model

Correspondence to:

H. Perfettini,
hugo.perfettini@ird.fr

Citation:

Perfettini, H., Frank, W. B., Marsan, D., & Bouchon, M. (2018). A model of aftershock migration driven by afterslip. *Geophysical Research Letters*, 45, 2283–2293. <https://doi.org/10.1002/2017GL076287>

Received 3 NOV 2017

Accepted 5 FEB 2018

Accepted article online 9 FEB 2018

Published online 10 MAR 2018

A Model of Aftershock Migration Driven by Afterslip

H. Perfettini¹, W. B. Frank^{2,3}, D. Marsan¹, and M. Bouchon¹

¹CNRS, IRD, ISTERRE, Université Grenoble Alpes, Grenoble, France, ²Department of Earth, Atmospheric, and Planetary Sciences, Massachusetts Institute of Technology, Cambridge, MA, USA, ³Now at Department of Earth Sciences, University of Southern California, Los Angeles, CA, USA

Abstract Aftershocks region have been extensively reported to expand logarithmically with time. The associated migration velocity is typically of the order of several km/decade but can be much larger, especially when observing early aftershock sequences, seismic swarms, or tremors. We present here a model for the expansion of aftershock zones based on the idea that aftershocks are triggered as afterslip grows with time along the fault. One of the model assumptions is that aftershocks are triggered when a critical level of afterslip is reached. We predict that the migration velocity V_p at time t following the mainshock is given by $V_p = \zeta \frac{A'}{\Delta\tau} \times \frac{c}{t}$, where A' is a frictional parameter, $\Delta\tau$ a characteristic value for the stress perturbation, c the radius of the stress perturbation, and ζ a constant of order unity. The scaling $V_p \propto 1/t$ implies a logarithmic expansion of the aftershock zone with time. The migration velocities predicted by our model are in quantitative agreement with the observations reported following aftershock sequence of small and large earthquakes in various tectonic settings, seismic swarms, and tremor sequences.

Plain Language Summary Aftershocks are shown to migrate with time away from the rupture area of the mainshock. This migration typically occurs as the logarithm of time. We present here a model based on the idea that afterslip drives aftershocks. The model is able to predict the migration as the logarithm of time, predicting apparent propagation velocities consistent with the observations. The propagation velocity is simply related to the physical parameters of the model.

1. Introduction

Aftershocks zones are known to expand with time (e.g., Chatelain et al., 1983; Henry & Das, 2001; Tajima & Kanamori, 1985). Thanks to the recent improvement of earthquake catalogs, a migration of the aftershock zone as the logarithm of time has been widely reported (Frank et al., 2017; Kato & Obara, 2014; Meng & Peng, 2016; Obana et al., 2014; Peng & Zhao, 2009; Tang et al., 2014; Wesson, 1987). Numerical simulations have suggested that this semilogarithmic migration is indicative of afterslip-driven aftershock activity (Ariyoshi et al., 2007; Kato, 2007) and subsequent observations have confirmed such (Peng & Zhao, 2009).

Assuming a rate strengthening rheology, Perfettini and Avouac (2004) showed that the temporal evolution of afterslip $U(t)$ is given by

$$U(t) = V_L t_r \log \left[1 + \frac{V_+}{V_L} \left(\exp \left(\frac{t}{t_r} \right) - 1 \right) \right] \tag{1}$$

where V_L is the long-term sliding (or loading) velocity after the mainshock, V_+ the sliding velocity right after the end of coseismic rupture, and t_r the duration of the postseismic phase. The parameters V_+ and t_r are given by

$$t_r = \frac{A'}{\dot{\tau}} \tag{2a}$$

$$A' = (a - b)\sigma \tag{2b}$$

$$V_+ = V_L \exp \left(\frac{\Delta CFS}{A'} \right) \tag{2c}$$

where $\dot{\tau}$ and ΔCFS are respectively the stressing rate and Coulomb stress change (induced by the mainshock) on the rate strengthening region, a and b the rate and state frictional parameters and σ the effective normal stress.

The sliding velocity $V(t) = \frac{dU}{dt}$ is given by

$$V(t) = \frac{V_+ \exp\left(\frac{t}{t_r}\right)}{1 + \frac{V_+}{V_L} \left[\exp\left(\frac{t}{t_r}\right) - 1 \right]} \quad (3)$$

Given that the duration of the aftershock sequence typically lasts for several years, for most practical use, the approximation $t \ll t_r$ in equation (1) is valid. In the case $t \ll t_r$, equation (1) simplifies into

$$U(t) \approx V_L t_r \log \left[1 + \frac{V_+}{V_L t_r} t \right], \quad t \ll t_r \quad (4)$$

while the sliding velocity reduces to

$$V(t) \approx \frac{V_+}{1 + \frac{V_+}{V_L t_r} t}, \quad t \ll t_r \quad (5)$$

Equation (4) is similar to the afterslip model of Marone et al. (1991).

Numerous studies have shown that postseismic deformation following moderate (Parkfield and l'Aquila earthquake sequences) and large earthquakes (Landers, Pisco, and Tohoku-Oki earthquake sequences) could be well described assuming only one component in the Principal Component Analysis (PCA) (Gualandi et al., 2016; Perfettini et al., 2010; Perfettini & Avouac, 2014; Savage & Langbein, 2008; Savage & Svarc, 1997). In other words, the afterslip distribution $U(\vec{r}, t)$ at position $\vec{r} = (x, y, z)$ and time t can be written as

$$U(\vec{r}, t) \approx f(\vec{r}) \times g(t) \quad (6)$$

where f and g are two functions, depending respectively uniquely on position \vec{r} and time t . Therefore, the afterslip distribution is described by the spatial pattern $f(\vec{r})$ and is modulated in time by the function $g(t)$. Typically, $g(t)$ predicts a logarithmic growth of afterslip with time and is well described by equation (4). Since the spatial and temporal evolution are independent, there is no propagation of afterslip in a literal sense ($U \propto h(\vec{r} - ct)$, where c is the propagation velocity).

Two extreme views can explain the production of aftershocks. In one (hereinafter Dieterich's model), aftershocks are produced by the response of a population of rate weakening patches to coseismic stress changes (Dieterich, 1994). In the other (hereinafter PA model), aftershocks are produced by afterslip loading the asperities that produce aftershocks (Perfettini & Avouac, 2004). In this case, the simplest assumption that could be made is that the seismicity rate $R(t)$, in a given area, is proportional to the rate of afterslip $V(t)$ at the same location. Consequently, and after use of equation (3), the seismicity rate is given by

$$R(t) = \frac{R_+ \exp\left(\frac{t}{t_r}\right)}{1 + \frac{R_+}{R_L} \left[\exp\left(\frac{t}{t_r}\right) - 1 \right]} \quad (7)$$

where R_L is the long-term seismicity rate after the mainshock, R_+ the seismicity rate right after the end of coseismic rupture, and t_r the duration of the postseismic phase. Again, the parameters t_r , A' and R_+ are given by

$$t_r = \frac{A'}{\dot{\epsilon}} \quad (8a)$$

$$A' = (a - b)\sigma \quad (8b)$$

$$R_+ = R_L \exp\left(\frac{\Delta CFS}{A'}\right) \quad (8c)$$

Surprisingly, both Dieterich and PA models predict exactly the same mathematical form for the evolution of the seismicity rate following a stress step (Perfettini & Avouac, 2004). One difference between both models is that, in Dieterich's model, A' should be replaced by $A = a\sigma$, where a the viscous parameter of the rate weakening patches.

Equation (7) predicts a $1/t$ decay of the seismicity rate $R(t)$ (Perfettini & Avouac, 2004) consistent with Omori's law (Omori, 1894). Utsu (1961) extended Omori's law proposing the modified Omori (or Omori-Utsu) law for which $R(t) = K(c + t)^{-p}$ where K is a constant, c is a characteristic time and p is the p value exponent. Dieterich and PA models correspond to the particular case $p = 1$ of the Omori-Utsu law, which is generally a good approximation.

Another major difference between both views is that PA's model has the additional constraint that the after-slip rate should be proportional to the seismicity rate, a feature that has been widely reported (Hsu et al., 2006; Perfettini & Avouac, 2004, 2007; Perfettini et al., 2005; Savage & Langbein, 2007, 2008). The A and A' parameters are usually found in the range 0.1–1 MPa. Considering the hydrostatic stress σ_H at 20 km depth, about 200 MPa, and $A = 0.1$ –1 MPa we find that $a = A/\sigma_H \approx 5 \times 10^{-4}$ – 5×10^{-3} . Although those values of a can be found in the laboratory (Ikari et al., 2016), they differ from typical laboratory estimates that fall between 10^{-3} and 10^{-2} .

The same calculation can be carried out in PA's model and implies that $a - b \approx 5 \times 10^{-4}$ – 5×10^{-3} . There is no contradiction in having the parameter $a - b$ being significantly smaller than the typical laboratory values of a and b . Another simple reason for a low value of $a - b$ is that velocity neutral regions ($a \approx b$) represent the regions that will show the strongest postseismic response, in agreement with equation (8c), and are the most likely to be studied (Frank et al., 2017).

2. Model of Aftershocks Migration

We consider a fault with only depth varying properties. Consequently, the normal stress, stressing rate, and rheological parameter A' can change with depth but are assumed to be laterally uniform. We will consider the migration of aftershocks along the strike direction x and assume that the initial Coulomb stress field vary with x , building the initial distribution of afterslip velocities. Consequently, the following variable dependencies are expected: $\dot{\epsilon}(z)$, $A'(z)$, $t_r(z)$, $\Delta CFS(x, z)$, and $V_{\pm}(x, z)$.

For a sake of simplicity, we will remain in the approximation $t \ll t_r$, focusing our attention on the early stage of the postseismic phase (typically several months after the mainshock). This period is when aftershock activity is the most intense. Considering later stages of the postseismic phase (typically several years) would require one to use the sliding velocity given by equation (3), instead of its approximation in equation (5) for $t \ll t_r$. Viscoelastic relaxation could also become dominant several years after the mainshock and become the dominant mode of postseismic deformation (Freymueller et al., 2000; Khazaradze et al., 2002).

Figure 1 shows a schematic sketch of the model. During the interseismic phase (Figure 1a), a population of asperities (dark blue patches) are loaded by the surrounding interseismic creep (yellow region), occurring at a steady state (plate) velocity. When the mainshock occurs (Figure 1b), some asperities slip coseismically (red patches), transferring large positive Coulomb stress into the nearby creeping regions. During the post-seismic phase (Figure 1c), the creeping regions loaded by the mainshock experience large amounts of afterslip (orange region). As this afterslip increases along the fault with time, aftershocks (light blue) are produced accordingly when a significant amount of afterslip (of the order of U_a given in equation (19)) accumulates.

Our model is consistent with the findings of Tajima and Kanamori (1985) that analyzed the aftershock expansion patterns of 44 large earthquakes. They explained their results using an asperity model of fault zones assuming that the fault plane is composed of "strong spots, called asperities (the locked regions of Figure 1a), and weak zones (the creeping regions of Figure 1a) surrounding asperities." They proposed that it is the gradual outward expansion of the stress changes caused by the mainshock in those weak zones that explain the expansion of aftershocks zones, a mechanism that corresponds to the growth of afterslip over the fault plane in our model (Figure 1c).

We will assume that the aftershocks directly triggered by coseismic stress changes only occur in the early stage of the postseismic phase (during, say, the first hours following the mainshock) and that their number represents a small fraction of the aftershocks triggered by afterslip.

2.1. Model Based on the Seismicity Model of Perfettini and Avouac (2004)

In Appendix A, we show that the characteristic aftershocks duration is

$$t_a = \frac{V_L}{V_+} t_r = \exp\left(-\frac{\Delta CFS}{A'}\right) t_r \quad (9)$$

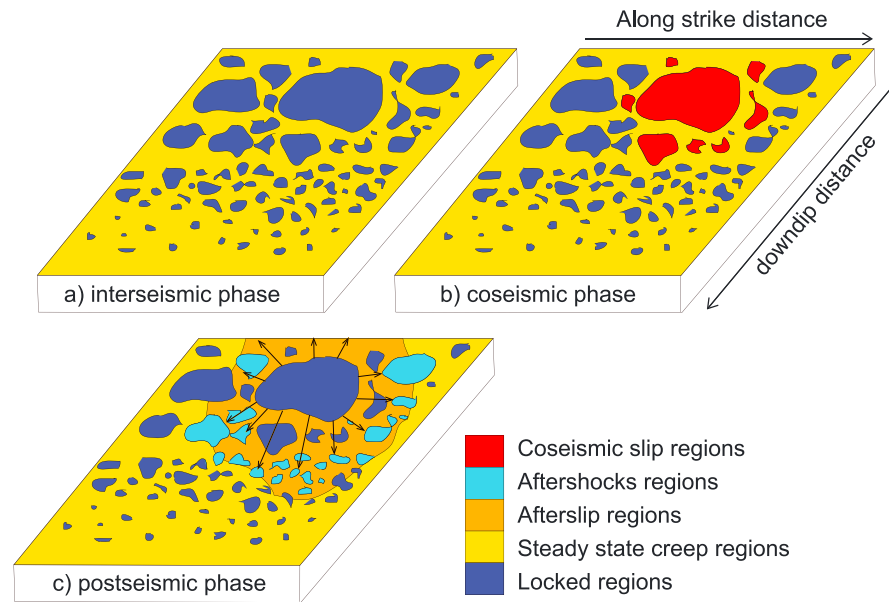


Figure 1. Schematic sketch of the model: (a) During the interseismic phase, a population of asperities (dark blue patches) are loaded by the surrounding interseismic creep (yellow region), occurring at a steady state (plate) velocity; (b) during the coseismic phase, some asperities slip coseismically (red patches), transferring large positive Coulomb stress into the nearby creeping regions; (c) during the postseismic phase, the creeping regions loaded by the mainshock show large amount of afterslip (orange region). As this afterslip increases along the fault with time, aftershocks (light blue) are produced accordingly when a significant amount of afterslip (of the order of U_a given in equation (19)) is reached. The black vectors describe the afterslip migration.

If $A' = (a - b)\sigma$ in PA's model is substituted by $A = a\sigma$, then equation (9) is exactly the aftershock duration time in Dieterich's model. So the following results will remain valid in Dieterich's model but A' needs to be substituted by A .

Equation (9) can be written as

$$t_a(x, z) = \exp\left(-\frac{\Delta\text{CFS}(x, z)}{A'(z)}\right) t_r(z) \quad (10)$$

Using equation (10), we have

$$\frac{\partial t_a}{\partial x} = -\frac{t_a}{A'} \frac{\partial \Delta\text{CFS}}{\partial x} \quad (11)$$

so that the propagation velocity $V_p = \frac{\partial x}{\partial t_a}$ is given by

$$V_p = \frac{A'}{t} \times \left(-\frac{\partial \Delta\text{CFS}}{\partial x}\right)^{-1} \quad (12)$$

Equation (12) shows that the smoother the Coulomb stress field (low Coulomb stress gradient), the higher the aftershock migration velocity V_p .

2.2. Model Based on a Slip Threshold

We will assume here that an aftershock is triggered when a critical level of afterslip U_a is reached on a nearby creeping patch. A rough estimate of this afterslip level will be given further in this section.

The slip front $U(x, t) = U_a$, initially at position x at time t , moves to a nearby position $x + dx$ at time $t + dt$. Since we are looking at the displacement of a constant slip level, then $U(x + dx, t + dt) = U(x, t) (= U_a)$ meaning that

$$dU = \frac{\partial U}{\partial x} dx + \frac{\partial U}{\partial t} dt = 0 \quad (13)$$

The propagation velocity $V_p = \frac{dx}{dt}$ is given by

$$V_p = -\frac{\frac{\partial U}{\partial t}}{\frac{\partial U}{\partial x}} \quad (14)$$

Taking equation (4) for U gives

$$\frac{\partial U}{\partial t} = \frac{V_+}{1 + \frac{V_+}{V_L t_r} t} \quad (15)$$

and

$$\frac{\partial U}{\partial x} = \frac{t}{1 + \frac{V_+}{V_L t_r} t} \times \frac{\partial V_+}{\partial x} = \frac{t}{A'} \times \frac{V_+}{1 + \frac{V_+}{V_L t_r} t} \times \frac{\partial \Delta CFS}{\partial x} \quad (16)$$

Using equations (15) and (16) together with (14) yields

$$V_p = \frac{A'}{t} \times \left(-\frac{\partial \Delta CFS}{\partial x} \right)^{-1} \quad (17)$$

Equation (17) is identical to (12) obtained considering the expansion of the aftershock zone. A direct correspondence between the two approaches can be drawn noting that the slip U_a accumulated during the characteristic aftershock duration t_a is of the order of $V_+ t_a$

$$U_a = V_+ t_a \quad (18)$$

Therefore, considering the expansion of the aftershocks zone is equivalent in following the migration of the constant slip level U_a . Using equations (2) and (9), (18) becomes

$$U_a = V_L t_r = \frac{V_L A'}{\dot{\epsilon}} \quad (19)$$

Assuming a typical duration of an aftershock sequence between 7 and 11 years (Parsons, 2002) and a loading velocity between 1 and 10 cm/yr imply that the slip level in the limit of the aftershock zone should stand between 0.07 and 1.10 m.

Equations (12) and (17) equivalently predict a decay of the propagation velocity as $1/t$. Between time t_i and time t , the aftershock zone R_a has expanded of an amount $\Delta R_a(t) = R_a(t) - R_a(t_i)$ given by

$$\Delta R_a(t) = A' \times \left(-\frac{\partial \Delta CFS}{\partial x} \right)^{-1} \log \left(\frac{t}{t_i} \right), t > t_i \quad (20)$$

which predicts an expansion as the logarithm of time.

Equation (20) is consistent with the conceptual model presented by Tajima and Kanamori (1985) to explain the difference of aftershock expansion patterns between “Mariana”- and “Chilean”-type subduction zones. In the “Mariana” type, small asperities are sparsely distributed while in the “Chilean” type, relatively large asperities are separated by small weak zones. In our model, this would correspond to a smooth coseismic Coulomb stress field (small Coulomb stress gradient) for the “Mariana” type, and a rougher one (large Coulomb stress gradient) for the “Chilean” type. Due to the $\left(-\frac{\partial \Delta CFS}{\partial x} \right)^{-1}$ term in equation (20), the corresponding expansion velocities would be larger for the “Mariana” type than for the “Chilean” type, consistent with the view of Tajima and Kanamori (1985).

3. Propagation Velocity Obtained Through Dimensional Analysis

Equations (17) and (20) giving respectively the propagation velocity and the extension of the aftershock zone both involve the gradient of the coseismic Coulomb stress changes with respect to the strike direction. The coseismic Coulomb stress field ΔCFS could be estimated using a kinematic slip model of the mainshock and knowing the elastic structure of the medium. Nevertheless, the obtained field could be significantly

different from the “real” coseismic Coulomb stress field. Assuming that the computed Coulomb stress field is approximate, its gradient will be even more approximate as the derivative will enhance the spatial fluctuations of the Coulomb stress field. Even though it might be appealing to evaluate $-1/\frac{\partial\Delta\text{CFS}}{\partial x}$ numerically, the corresponding estimate will likely be far from its true value.

On the contrary, a simple dimensional analysis allows a qualitative estimate of the mean gradient in Coulomb stress

$$\left\langle \frac{\partial\Delta\text{CFS}}{\partial x} \right\rangle \approx -\frac{1}{\zeta} \frac{\Delta\tau}{c} \quad (21)$$

where $\Delta\tau$ and c are respectively the stress drop and characteristic size of the mainshock, ζ is a constant of order unity while $\langle \dots \rangle$ means spatial (along strike) average. Note that in equation (21), the minus sign comes from the fact that the Coulomb stress field decreases with increasing distance from the rupture area.

Using equation (21), we obtain

$$\left\langle -\left(\frac{\partial\Delta\text{CFS}}{\partial x}\right)^{-1} \right\rangle = \zeta \frac{c}{\Delta\tau} \quad (22)$$

In Appendix B, we show that for the idealized Coulomb stress field proposed by Dieterich (1994), $\zeta = 2.77$.

Introducing equations (22) into (17) and (20), we obtain

$$V_p = \zeta \frac{A'}{t} \times \frac{c}{\Delta\tau} \quad (23)$$

and

$$\Delta R_a(t) = \zeta A' \times \frac{c}{\Delta\tau} \log\left(\frac{t}{t_i}\right), \quad t > t_i \quad (24)$$

Finally, the velocity per decade $V_{p/d}$ often reported in the literature is given by $\frac{\Delta R_a(t)}{\log 10}$ and $\frac{t}{t_i} = 10$ leading to

$$V_{p/d} = \zeta A' \frac{c}{\Delta\tau} \quad (25)$$

Using equation (25), equations (23) and (24) become

$$V_p = \frac{V_{p/d}}{t} \quad (26a)$$

$$\Delta R_a(t) = V_{p/d} \times \log\left(\frac{t}{t_i}\right), \quad t > t_i \quad (26b)$$

It follows that the velocity per decade $V_{p/d}$ characterizes the magnitude of the aftershocks migration.

4. Comparison to Aftershocks Sequences

4.1. The 2015 M_w 8.3 Illapel Earthquake

We will show here how to apply our model to the case of the aftershocks of the 2015 M_w 8.3 Illapel Earthquake in Central Chile. For this aftershock sequence, Frank et al. (2017) found $A' \approx 3.5 \times 10^{-2}$ MPa and $\Delta\tau \approx 0.24$ MPa based on the coseismic slip model of Ruiz et al. (2016), and $A' \approx 4.5 \times 10^{-2}$ MPa and $\Delta\tau \approx 0.3$ MPa based on the coseismic slip model of Shrivastava et al. (2016).

The equivalent source radius c can be obtained assuming a circular crack for which (equation (4.30) of Scholz, 2002)

$$c = \left(\frac{7}{16} \frac{M_0}{\Delta\tau}\right)^{\frac{1}{3}} \quad (27)$$

Assuming $M_0 = 3.55 \times 10^{21}$ N m which corresponds to a M_w 8.3 earthquake, equation (27) yields $c \approx 186$ km and 173 km for the coseismic models of Ruiz et al. (2016) and Shrivastava et al. (2016), respectively.

The parameters A' , $\Delta\tau$, and c being determined, we can use equation (24) to predict the expansion of the aftershocks zone once the constant ζ is known. Figure 2 shows the expansion of the aftershock zone using

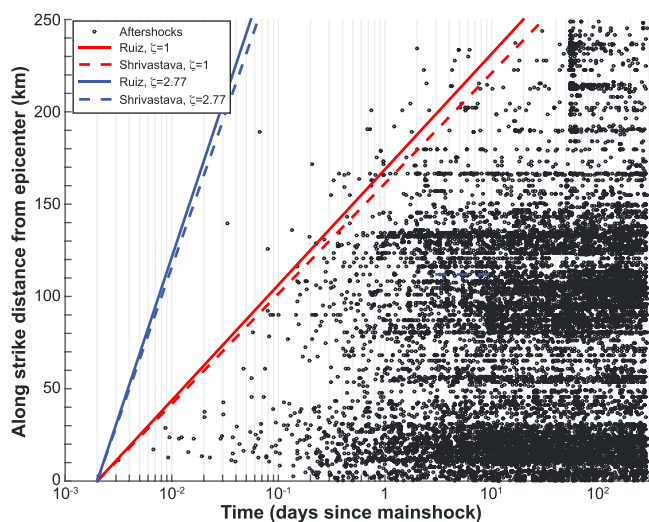


Figure 2. Along-strike expansion of the aftershock zone of the Illapel earthquake predicted by equation (24) considering the coseismic slip models of Ruiz et al. (2016) (solid line) and Shrivastava et al. (2016) (dashed line) for $\zeta = 1$ (blue lines) and $\zeta = 2.77$ (red lines). The aftershock zone shows an expansion as the logarithm of time. The plotted data are from Frank et al. (2017).

4.2. Other Migration Sequences

4.2.1. Californian Earthquakes

Figure 3 adapted from Marsan and Lengliné (2008) shows the characteristic aftershock migration pattern in California (open circles). The mean epicentral distance from a mainshock to its aftershocks (both direct and indirect aftershocks, see Marsan & Lengliné, 2008, for further details) is computed as a function of time. The mean is taken by considering all possible $m \geq 3$ mainshocks, for southern California earthquakes from 1984 to 2002. The solid line in Figure 3 corresponds to the best fit model (solid line) of equation (26b), corresponding to $V_{p/d} \approx 3.15$ km/decade.

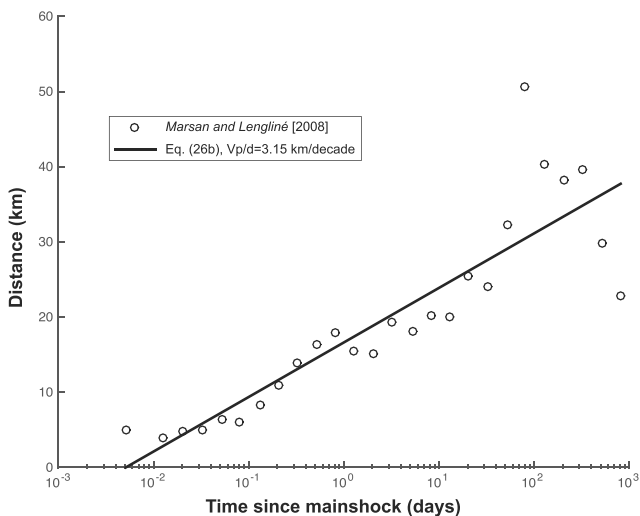


Figure 3. Characteristic expansion of aftershocks (square) in California (Marsan & Lengliné, 2008) together with a logarithmic fit (straight line) obtained considering equation (2009b) with $V_{p/d} \approx 3.15$ km/decade. The plotted data are from Marsan and Lengliné (2008).

equation (24) between $t = 10^2 - 10^7$ s and the values of A' reported above, the parameter t_i being set to the time of the first observation ($t_i = 10^2$ s). In Figure 2, equation (24) has been used considering the coseismic models of Ruiz et al. (2016) (solid line) and Shrivastava et al. (2016) (dashed line) and assuming $\zeta = 1$ (red lines) or $\zeta = 2.77$ (blue lines). For both values of $\zeta = 1$ and 2.77, Figure 2 is in qualitative agreement with the observed migration of aftershocks reported by Frank et al. (2017), justifying the use of equation (24) with a constant ζ of order unity.

The straight lines in Figure 2 (showing the along-strike distance of aftershocks as a function of the logarithm of time) correspond to the position of the afterslip front as a function of time, and whose amplitude is roughly given by U_a from equations (18) or (19). In our model, locked asperities close to rupture (i.e., at the end of their loading cycle) will tend to rupture instantaneously when reached by the afterslip front, and no aftershocks will occur before the arrival of this front. The asperities further from failure might rupture some time after the passage of the afterslip front, depending on their state in the loading cycle. In other words, the spread of the data simply reflects the variability in nucleation time of the asperities, depending on their size, stress history, etc.

For both values of $\zeta = 1$ and 2.77, Figure 2 shows that the aftershocks zone expands as the logarithm of time, as observed in numerous aftershock sequences (Frank et al., 2017, and references therein).

For a mainshock of moment magnitude $M_0 = 1.26 \times 10^{18}$ N m ($M_w 6.0$) and assuming $A' = 0.5$ MPa as in Perfettini and Avouac (2007) and $\Delta\tau \approx 2.3$ MPa (Kim & Dreger, 2008), we find using equation (25) and $\zeta = 1$ that $V_{p/d} \approx 1.35$ km/decade. Considering the value $\zeta \approx 2.77$ found in Appendix B, we find $V_{p/d} \approx 3.74$ km/decade. For a mainshock of moment magnitude $M_0 = 3.98 \times 10^{19}$ N m ($M_w 7.0$) with $A' = 0.5$ MPa and $\Delta\tau \approx 2.3$ MPa, we get $V_{p/d} \approx 4.27$ km/decade when $\zeta = 1$ and $V_{p/d} \approx 11.8$ km/decade when $\zeta = 2.77$. The value of about 3 km/decade found in Figure 3 is consistent with the values predicted by our model.

4.2.2. The 2011 $M_w 9.0$ Tohoku-Oki Earthquake

Lengliné et al. (2012) reported an early expansion of the aftershock zone as the logarithm of time. Based on their Figure 4, the migration velocity is of the order of 100 km/decade. Using $\Delta\tau = 2.4$ MPa as the mean stress drop of the Tohoku earthquake (Brown et al., 2015), we find, using equation (25) with $\zeta = 2.77$ (see Appendix B), that $V_{p/d} \approx 112$ km/decade for $A' = 0.5$ MPa and $V_{p/d} \approx 11.2$ km/decade for $A' = 5 \times 10^{-2}$ MPa. Our model suggests in the region of the Tohoku earthquake, the parameter A' is probably closer to the value 0.5 MPa than to the value $A' = 4 \times 10^{-2}$ MPa found by Frank et al. (2017) for the Central Chile subduction zone.

Kato et al. (2014) reported the propagation of events within a seismic swarm triggered by the Tohoku-Oki earthquake, with a migration velocity over

2 days of about 20 km/d. Using equation (23) with $\Delta\tau = 2.4$ MPa, $A' = 0.5$ MPa as suggested earlier gives $V_p \approx 55.9$ km/d for $t = 2$ day, in quantitative agreement with the observations of Kato et al. (2014).

5. Conclusion

Our simple model only considers along-strike migration. If propagation with depth is considered, then all spatial derivatives should also apply on t , and $\dot{\tau}$ and not only on V_+ and ΔCFS . However, we believe that the simple scaling proposed should be general although the value of the constant ζ depends on the real Coulomb stress distribution which is unknown. It also depends on the real source extent that we have assumed circular here for simplicity. Nevertheless, our analysis of section 4.1 and Appendix B suggests that the constant ζ should be of the order unity.

Our model can explain the gross features of the migration of aftershock zones: (1) an expansion as the logarithm of time and equivalently a migration rate decaying as the inverse of time, (2) migration velocities typically of the order of several km/decade. Initial migration speed should be large due to the 1/time scaling predicted by our model, consistent with the large migration speeds reported following seismic swarms (Shelly et al., 2011).

In practice, equation (23) can help estimating the order of magnitude of the A' parameter. Indeed, in each cases, a rough estimate of $\Delta\tau$ and c is possible. $\Delta\tau$ represents the characteristic amplitude of the perturbation, for instance the average stress drop of the mainshock when considering an aftershock sequence. For aftershock sequences, the source radius c of the stress perturbation can be roughly estimated using equation (27) or by considering the average radius outlined by the early aftershocks. So once the characteristic observation time t is given and the migration velocity V_p is known, equation (23) can be used to infer a rough estimate of A' .

When applied to the case of the Illapel earthquake, equation (23) was more constrained as the model parameters $\Delta\tau$, c , and A' were previously estimated (Frank et al., 2017). Assuming ζ of order unity, our model predictions are consistent with the observations. Consequently, our modeling approach based on the idea that afterslip drives seismicity can simultaneously adjust the aftershock distribution in depth as done in Frank et al. (2017), together with explaining the migration of aftershocks with time, using the exact same value of the A' parameter in both cases. We believe that our results strengthen the idea that afterslip drives aftershocks as postulated in Perfettini and Avouac (2004, 2007).

The assumption that the resisting stress τ depends positively on the logarithm of the sliding velocity seems to be robust as it agrees with the evolution of postseismic surface deformation, aftershock activity, and how seismicity migrates with time in response to an aseismic creep burst. Avouac (2015) showed that the common observation that postseismic surface displacements evolve as the logarithm of time naturally implies that the postseismic stress acting on the fault increases as the logarithm of the fault sliding velocity.

A logarithmic rate strengthening rheology is characteristic of numerous thermally activated processes (e.g., Eyring, 1935) such as dislocation creep, diffusion creep, and pressure solution creep. Stress corrosion might also fall into the same class of deforming mechanisms. Stress corrosion in regions of high stress following the mainshock has been proposed to be a viable mechanism to explain the production of aftershocks (Das & Scholz, 1981; Scholz, 1968). This theory implies a decaying rate of aftershocks with the inverse of time, as does our model. In stress corrosion theory, the expression of the mean time to fracture $\langle t \rangle$, used to evaluate the probability of aftershock production, is proportional to $\exp(-\tau/\chi)$, where χ is a temperature and material dependent constant (Scholz, 1968). As the mean sliding velocity V of the interface scales as $V \propto 1/\langle t \rangle$, then $V \propto \exp(\tau/\chi)$ is expected. Consequently, we cannot exclude the possibility that the physical mechanism driving aftershocks is stress corrosion and not frictional afterslip.

In this paper, we have assumed that the evolution of afterslip is governed by rate and state friction, but our results would remain unchanged considering any type of thermally activated processes such as those mentioned above. The only requirement for our results to hold is that the shear stress τ and the deformation rate $\dot{\epsilon}$ should be such that $\dot{\epsilon} \propto \exp(\tau/c)$, where $c > 0$ is a constant that is analogous to the parameter A' of our model.

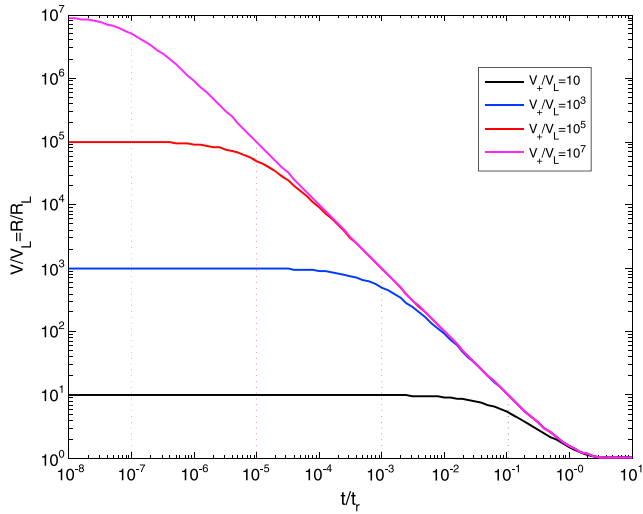


Figure A1. Normalized seismicity and afterslip rates as a function of normalized time for various initial sliding velocities $V_+/V_L = 10$ (black curve), 10^3 (blue curve), 10^5 (red curve), and 10^7 (magenta curve). The total aftershock (or afterslip) duration is t_r and the characteristic aftershock (afterslip) duration t_a is given by the dotted vertical lines.

Appendix A: Determination of the Duration of the Aftershock Sequence

Figure A1 shows the normalized seismicity and afterslip rates as a function of normalized time for various initial sliding velocities $V_+/V_L = 10$ (black curve), 10^3 (blue curve), 10^5 (red curve), and 10^7 (magenta curve). The afterslip or seismicity rate shows a plateau of characteristic duration t_a , followed by a decay as $1/t$ before returning to a steady state regime. Clearly, the total aftershock (or afterslip) duration is t_r and is independent of the initial sliding velocity.

The characteristic duration of the aftershocks (afterslip) sequence can be obtained finding the intersection of the sliding velocity V_∞ corresponding to an infinite initial velocity (limit $V_+/V_L \rightarrow \infty$ in equation (3))

$$V_\infty(t) = V_L \times \frac{\exp\left(\frac{t}{t_r}\right)}{\exp\left(\frac{t}{t_r}\right) - 1} \quad (A1)$$

with the initial velocity V_+ . Setting $V_\infty(t_a) = V_+$ in equation (A1) gives

$$t_a = t_r \times \log\left[\frac{1}{1 - \frac{V_+}{V_L}}\right] \quad (A2)$$

In the most common cases $V_+ \gg V_L$ and equation (A2) becomes

$$t_a = t_r \frac{V_+}{V_L} = t_r \exp\left(-\frac{\Delta CFS}{A'}\right) \quad (A3)$$

which is identical to equation (18) of Dieterich (1994) (after substitution of A' by $A = a\sigma$ in Dieterich's model) for the aftershock duration time (named t_a in Dieterich, 1994).

Appendix B: Determination of the Constant ζ in the Case of a Simplified Coseismic Coulomb Stress Change

Following Dieterich (1994), we consider the following Coulomb stress changes along the strike direction x

$$\Delta CFS(x) = \Delta\tau \left[\left(1 - \frac{c^3}{x^3}\right)^{-\frac{1}{2}} - 1 \right], \quad x > c \quad (B1)$$

where c is the radius of the coseismic rupture, $\Delta\tau > 0$ the absolute value of the mean coseismic stress drop. As mentioned by Dieterich (1994), this idealized Coulomb stress field "does not represent azimuthal dependencies" on the Coulomb stress "but it does incorporate both the square root stress singularity at the crack tip and the stress falloff by $1/x^3$ at larger distances which are characteristic of cracks in an elastic medium."

Using equation (B1), the stress gradient (the derivative of the Coulomb stress field with respect to along-strike distance) is given by

$$\frac{\partial \Delta CFS(x)}{\partial x} = -\frac{3c^3 \Delta\tau}{2x^4 \left(1 - \frac{c^3}{x^3}\right)^{\frac{3}{2}}}, \quad x > c \quad (B2)$$

which yields

$$\left(-\frac{\partial \Delta CFS}{\partial x}\right)^{-1} = \frac{2x^4}{3c^3 \Delta\tau} \left(1 - \frac{c^3}{x^3}\right)^{\frac{3}{2}}, \quad x > c \quad (B3)$$

For practical use, we will consider the mean value of equation (B3), averaged over c and $2c$ (the stress changes at twice the source radius and beyond becomes negligible, see Figure B1)

$$\left\langle \left(-\frac{\partial \Delta CFS}{\partial x}\right)^{-1} \right\rangle = \frac{1}{c} \int_c^{2c} \left(-\frac{\partial \Delta CFS}{\partial x}\right)^{-1} dx \quad (B4)$$

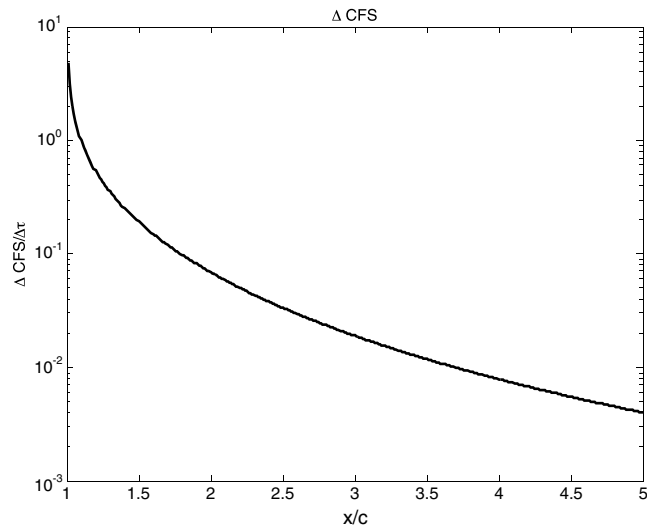


Figure B1. Coulomb stress change predicted by equation (B1) from Dieterich (1994), where c is the source radius and $\Delta\tau$ the amplitude of the stress drop of the mainshock.

After introduction of the variable $u = x/c$, we have

$$\frac{1}{c} \times \int_c^{2c} \frac{2x^4}{3c^3} \left(1 - \frac{c^3}{x^3}\right)^{\frac{3}{2}} dx = \zeta \times c \quad (B5)$$

with

$$\zeta = \frac{2}{3} \int_1^2 u^4 (1 - u^{-3})^{\frac{3}{2}} du \approx 2.77 \quad (B6)$$

Combining equation (B4) together with (B3), (B5), and (B6) yields

$$\left\langle - \left(\frac{\partial \Delta CFS}{\partial x} \right)^{-1} \right\rangle = \zeta \times \frac{c}{\Delta\tau} \quad (B7)$$

Note that the constant ζ depends on the real Coulomb stress field and the value given in equation (B6) is obtained considering an idealized loading profile. Nevertheless, the scaling proposed in equation (23) should remain valid for realistic stress changes as $\left\langle - \left(\frac{\partial \Delta CFS(x)}{\partial x} \right)^{-1} \right\rangle$ scales as $\frac{c}{\Delta\tau}$, and ζ should be taken as an adjustable constant of order unity.

Acknowledgments

W. B. F. was supported by NSF grant EAR-PF 1452375. We thank C. Marone and an anonymous reviewer for their thoughtful reviews that have helped improve the manuscript. The data used to produce Figures 2 and 3 are from previously published work.

References

- Ariyoshi, K., Matsuzawa, T., & Hasegawa, A. (2007). The key frictional parameters controlling spatial variations in the speed of postseismic-slip propagation on a subduction plate boundary. *Earth and Planetary Science Letters*, *256*, 136–146.
- Avouac, J.-P. (2015). From geodetic imaging of seismic and aseismic fault slip to dynamic modeling of the seismic cycle. *Annual Review of Earth and Planetary Sciences*, *43*, 233–271.
- Brown, L., Wang, K., & Sun, T. (2015). Static stress drop in the M_w 9 Tohoku-oki earthquake: Heterogeneous distribution and low average value. *Geophysical Research Letters*, *42*, 10,595–10,600. <https://doi.org/10.1002/2015GL066361>
- Chatelain, J., Cardwell, R., & Isacks, B. (1983). Expansion of the aftershock zone following the Vanuatu (New Hebrides) earthquake on 15 July 1981. *Geophysical Research Letters*, *10*, 385–388.
- Das, S., & Scholz, C. (1981). Theory of time-dependent rupture in the Earth. *Journal of Geophysical Research*, *86*, 6039–6051.
- Dieterich, J. H. (1994). A constitutive law for rate of earthquake production and its application to earthquake clustering. *Journal of Geophysical Research*, *99*, 2601–2618.
- Eyring, H. (1935). High fluid pressures during regional metamorphism and deformation: Implications for mass transport and deformation mechanisms. *Journal of Chemical Physics*, *3*, 107–115.
- Frank, W. B., Poli, P., & Perfettini, H. (2017). Mapping the rheology of the Central Chile subduction zone with aftershocks. *Geophysical Research Letters*, *44*, 5374–5382. <https://doi.org/10.1002/2016GL072288>
- Frey Mueller, J., Cohen, S., & Fletcher, H. (2000). Spatial variations in present-day deformation, Kenai Peninsula, Alaska, and their implications. *Journal of Geophysical Research*, *105*, 8079–8101.
- Gualandi, A., Avouac, J.-P., Galetzki, J., Genrich, J. F., Blewitt, G., Bijaya Adhikari, L., et al. (2016). Pre- and post-seismic deformation related to the 2015, M_w 7.8 Gorkha earthquake, Nepal. *Tectonophysics*, *714*, 90–106. <https://doi.org/10.1016/j.tecto.2016.06.014>
- Henry, C., & Das, S. (2001). Aftershock zones of large shallow earthquakes: Fault dimensions, aftershock area expansion and scaling relations. *Geophysical Journal International*, *147*, 272–293.

- Hsu, Y.-J., Simons, M., Avouac, J.-P., Galtezka, J., Sieh, K., Chlieh, M., et al. (2006). Frictional afterslip following the 2005 Nias-Simeulue Earthquake, Sumatra. *Science*, *312*, 1921–1926.
- Ikari, M., Carpenter, B., & Marone, C. (2016). A microphysical interpretation of rate- and state-dependent friction for fault gouge. *Geochemistry, Geophysics, Geosystems*, *17*, 1660–1677. <https://doi.org/10.1002/2016GC006286>
- Kato, A., & Obara, K. (2014). Step-like migration of early aftershocks following the 2007 M_w 6.7 Noto-Hanto earthquake, Japan. *Geophysical Research Letters*, *41*, 3864–3869. <https://doi.org/10.1002/2014GL060427>
- Kato, A., Igarashi, T., & Obara, K. (2014). Detection of a hidden Boso slow slip event immediately after the 2011 M_w 9.0 Tohoku-Oki earthquake, Japan. *Geophysical Research Letters*, *41*, 5868–5874. <https://doi.org/10.1002/2014GL061053>
- Kato, N. (2007). Expansion of aftershock areas caused by propagating post-seismic sliding. *Geophysical Journal International*, *168*, 797–808.
- Khazaradze, G., Wang, K., Klotz, J., Hu, Y., & He, J. (2002). Prolonged post-seismic deformation of the 1960 great Chile earthquake and implications for mantle rheology. *Geophysical Research Letters*, *29*(22), 2050. <https://doi.org/10.1029/2002GL015986>
- Kim, A., & Dreger, D. S. (2008). Rupture process of the 2004 Parkfield earthquake from near-fault seismic waveform and geodetic records. *Journal of Geophysical Research*, *113*, B07308. <https://doi.org/10.1029/2007JB005115>
- Lengliné, O., Enescu, B., Peng, Z., & Shiomi, K. (2012). Decay and expansion of the early aftershock activity following the 2011, M_w 9.0 Tohoku earthquake. *Geophysical Research Letters*, *39*, L18309. <https://doi.org/10.1029/2012GL052797>
- Marone, C. J., Scholz, C. H., & Bilham, R. (1991). On the mechanics of earthquake afterslip. *Journal of Geophysical Research*, *96*, 8441–8452.
- Marsan, D., & Lengliné, O. (2008). Extending earthquakes' reach through cascading. *Science*, *319*, 1076–1079.
- Meng, X., & Peng, Z. (2016). Increasing lengths of aftershock zones with depths of moderate-size earthquakes on the San Jacinto Fault suggests triggering of deep creep in the middle crust. *Geophysical Journal International*, *204*, 250–261. <https://doi.org/10.1093/gji/ggv445>
- Obana, K., Takahashi, T., No, T., Kaiho, Y., Kodaira, S., Yamashita, M., et al. (2014). Distribution and migration of aftershocks of the 2010 M_w 7.4 Ogasawara Islands intraplate normal-faulting earthquake related to a fracture zone in the Pacific plate. *Geochemistry, Geophysics, Geosystems*, *15*, 1363–1373. <https://doi.org/10.1002/2014GC005246>
- Omori, F. (1894). On the after-shocks of earthquakes. *Journal of Colloid Science*, *7*, 111–200.
- Parsons, T. (2002). Global Omori law decay of triggered earthquakes: Large aftershocks outside the classical aftershock zone. *Journal of Geophysical Research*, *107*(B9), 2199. <https://doi.org/10.1029/2001JB000646>
- Peng, Z., & Zhao, P. (2009). Migration of early aftershocks following the 2004 Parkfield earthquake. *Nature Geoscience*, *2*, 877–881.
- Perfettini, H., & Avouac, J.-P. (2004). Postseismic relaxation driven by brittle creep: A possible mechanism to reconcile geodetic measurements and the decay rate of aftershocks, application to the Chi-Chi earthquake, Taiwan. *Journal of Geophysical Research*, *109*, B02304. <https://doi.org/10.1029/2003JB002488>
- Perfettini, H., & Avouac, J.-P. (2007). Modeling afterslip and aftershocks following the 1992 Landers Earthquake. *Journal of Geophysical Research*, *112*, B07409. <https://doi.org/10.1029/2006JB004399>
- Perfettini, H., & Avouac, J.-P. (2014). The seismic cycle in the area of the 2011 M_w 9.0 Tohoku-Oki earthquake. *Journal of Geophysical Research: Solid Earth*, *119*, 4469–4515. <https://doi.org/10.1002/2013JB010697>
- Perfettini, H., Avouac, J.-P., & Ruegg, J. (2005). Geodetic displacements and aftershocks following the 2001, M_w = 8.4 Peru earthquake: Implications for the mechanics of the earthquake cycle along subduction zones. *Journal of Geophysical Research*, *109*, B09404. <https://doi.org/10.1029/2004JB003522>
- Perfettini, H., Avouac, J.-P., Tavera, H., Kositsky, A., Nocquet, J.-M., Bondoux, F., et al. (2010). Seismic and aseismic slip on the Central Peru megathrust. *Nature*, *465*, 78–81. <https://doi.org/10.1038/nature09062>
- Ruiz, S., Klein, E., Campo, F. d., Rivera, E., Poli, P., Metois, M., et al. (2016). The seismic sequence of the 16 September 2015 M_w 8.3 Illapel, Chile, Earthquake. *Seismological Research Letters*, *87*(4), 789–799. <https://doi.org/10.1785/0220150281>
- Savage, J., & Langbein, J. (2007). Postearthquake relaxation and aftershock accumulation linearly related after 2003 Chengkung (M 6.5, Taiwan) and 2004 Parkfield (M 6.0 California) earthquakes. *Bulletin of the Seismological Society of America*, *97*(5), 1632–1645. <https://doi.org/10.1785/0120070069>
- Savage, J., & Langbein, J. (2008). Postearthquake relaxation after the 2004 M 6 Parkfield, California earthquake and rate-and-state friction. *Journal of Geophysical Research*, *113*, B10407. <https://doi.org/10.1029/2008JB005723>
- Savage, J., & Svarc, J. (1997). Postseismic deformation associated with the 1992 M_w = 7.3 Landers earthquake, southern California. *Journal of Geophysical Research*, *102*, 7565–7577.
- Scholz, C. (1968). Microfractures, aftershocks, and seismicity. *Bulletin of the Seismological Society of America*, *58*, 1117–1130.
- Scholz, C. H. (2002). *The mechanics of earthquakes and faulting*. New York: Columbia University Press.
- Shelly, D. R., Peng, Z., Hill, D. P., & Aiken, C. (2011). Triggered creep as a possible mechanism for delayed dynamic triggering of tremor and earthquakes. *Nature Geoscience*, *4*, 384–388. <https://doi.org/10.1038/NGEO1141>
- Shrivastava, M. N., González, G., Moreno, M., Chlieh, M., Salazar, P., Reddy, C. D., et al. (2016). Coseismic slip and afterslip of the 2015 M_w 8.3 Illapel (Chile) earthquake determined from continuous GPS data. *Geophysical Research Letters*, *43*, 10,710–10,719. <https://doi.org/10.1002/2016GL070684>
- Tajima, F., & Kanamori, H. (1985). Global survey of aftershock area expansion patterns. *Physics of the Earth and Planetary Interiors*, *40*, 77–134.
- Tang, C.-C., Lin, C.-H., & Peng, Z. (2014). Spatial-temporal evolution of early aftershocks following the 2010 M_L 6.4 Jiashian earthquake in southern Taiwan. *Geophysical Journal International*, *199*, 1772–1783.
- Utsu, T. (1961). A statistical study on the occurrence of aftershocks. *Geophysical Magazine*, *30*, 521–605.
- Wesson, R. L. (1987). Modelling aftershock migration and afterslip of the San Juan Bautista, California, earthquake of October 3. *Tectonophysics*, *144*, 215–229.